Technical Paper
J. Astron. Space Sci. 32(1), 91-99 (2015)
http://dx.doi.org/10.5140/JASS.2015.32.1.91

JASS Journal of Astronomy and Space Sciences

Burst Locating Capability of the Korean Solar Radio Burst Locator (KSRBL)

Jung-Eun Hwangbo[1,2†], Su-Chan Bong[1,3], Sung-Hong Park[4], Dae-Young Lee[2], Kyung-Suk Cho[1,3], Jaejin Lee[1,3], Young-Deuk Park[1]

[1]Korea Astronomy and Space Science Institute, Daejeon 305-348, Korea
[2]Department of Astronomy and Space Science, Chungbuk National University, Cheongju ,Korea
[3]Astronomy and Space Science Major, University of Science and Technology, Daejeon ,Korea
[4]National Observatory of Athens, Thiseio Athens 11810, Greece

The Korean Solar Radio Burst Locator (KSRBL) is a solar radio spectrograph observing the broad frequency range from 0.245 to 18 GHz with the capability of locating wideband gyrosynchrotron bursts. Due to the characteristics of a spiral feed, the beam center varies in a spiral pattern with frequency, making a modulation pattern over the wideband spectrum. After a calibration process, we obtained dynamic spectra consistent with the Nobeyama Radio Polarimeter (NoRP). We compared and analyzed the locations of bursts observed by KSRBL with results from the Nobeyama Radioheliograph (NoRH) and Atmospheric Imaging Assembly (AIA). As a result, we found that the KSRBL provides the ability to locate flaring sources on the Sun within around 2′.

Keywords: solar flare, solar radio burst, solar microwave burst, burst locator

1. INTRODUCTION

Since solar radio emissions were first discovered (Appleton & Hey 1946), they have been regarded as an important subject not only for scientific investigations but also for the examination of space weather effects such as radio interference. Various research results (Bala et al. 2002, Nita et al. 2002, Gary et al. 2004, Nita et al. 2004a, Cerruti et al. 2006, 2008, Carrano et al. 2009) have demonstrated how wireless communications and navigation systems such as cellular phones, their stations, and the Global Positioning System (GPS) can be easily affected by strong solar radio emissions, especially when there are strong radio bursts during sunrise and sunset.

This solar activity is often accompanied by bursts of solar energetic particles (SEPs), coronal mass ejections (CMEs), shock waves, X-ray and UV radiations. Those events also affect space weather (Feynman & Gabriel 2000). The location of solar events is important, because the location determines whether and to what degree the earth will be impacted: for example, the effect of SEPs are highly dependent on the longitude of the Sun where the activity originates (Park & Moon 2014, Dierckxsens et al. 2015). By monitoring the location of solar events, we can be prepared for potential damages caused by accelerated particles from the solar burst. For example, we can shut down the power supply of a spacecraft for a short time to prevent damage, even though we can't stop the solar storm.

Many spectrometry instruments have been developed throughout the world over many years to study and monitor the solar radio bursts, and with changing technology their performance has advanced greatly. There are several broadband spectrometers, such as those operating at 18–1800 MHz in Culgoora and Learmonth, Australia; the Zurich (ETH) spectrometer (Messmer et al. 1999) operating at 0.1–4 GHz in Switzerland; and the spectrometer operating in five different wave bands (0.7–1.5 GHz, 1.0–2.0 GHz, 2.6–3.8 GHz, 4.5–7.5 GHz, and 5.2–7.6 GHz, respectively) at

Received Feb 12, 2015 **Revised** Mar 9, 2015 **Accepted** Mar 10, 2015
†**Corresponding Author**
E-mail:hwangbo@kasi.re.kr, ORCID: 0000-0002-1296-1541
Tel: +82-42-865-2028, Fax: +82-42-865-3358

Beijing, Kunming, and Nanjing, China (Fu et al. 2004). To cover a broader overall spectral range, other instruments operate at discrete frequencies, such as the Nobeyama Radiopolarimeter (NoRP) (1, 2, 3.8, 9.4, 17, 35, and 80 GHz) in Japan (Nakajima et al. 1985), and the US Air Force Radio Solar Telescope Network (RSTN) (0.245, 0.410, 0.606, 1.4, 2.7, 5.0, 8.8, and 15 GHz) at four sites around the world (Guidice et al. 1981). The goal of all of these instruments is to cover as broad a range of radio frequencies as possible, with the highest spectral and temporal resolutions possible (Dou et al. 2009).

The instrument described in this study, the Korean Solar Radio Burst Locator (KSRBL), combines locating ability with the capabilities of a broadband spectrometer, to provide continuous spectral coverage from 245 MHz to 18 GHz, with an instantaneous bandwidth of 2 GHz. This is made possible by recent advances in high-speed digital signal processing based on field programmable gate arrays (FPGAs).

Radio emissions can be classified largely into two categories: the slowly varying quiet sun emissions, and the abrupt radio bursts. Of these two categories, the radio bursts associated with solar flares have been observed in a wide range of wavelengths from millimeter to decameter by using ground based instruments. The characteristics of the bursts vary with wavelength. Solar microwave observations at frequencies of 1-20 GHz (1.5-30 cm) are used to study the characteristics of hot plasma (thermal emission) and nonthermal high energy electrons (gyrosynchrotron emission) in the upper chromosphere and the corona (Bastian 2005). The microwave bursts are known to be caused by gyrosynchrotron emissions due to energetic electrons moving in a strong magnetic field. Their spectra often show impulsive and gradual emission patterns. Overall intensity, duration and spectral hardness are known to correlate with the kinetics of energetic electrons.

In this case, the energetic electrons are being rapidly accelerated and transported in the course of instantaneous energy releases from magnetic reconnections accompanying flares. To understand the electron acceleration and transport in solar flares in more detail, we need a highly efficient instrument such as the KSRBL, with high temporal and spectral resolution (Hwangbo et al. 2014).

This paper begins with an introduction to, and the system configuration of, the KSRBL in Section 2. Section 3 shows the daily operation and the calibration. As a main result, we evaluate the ability of the KSRBL to locate bursts, in Section 4. We summarize our results and conclude in Section 5 with KSRBL's potential for operational space weather monitoring and scientific discoveries.

Fig. 1. The Korean Solar Radio Burst Locator (KSRBL).

2. KOREAN SOLAR RADIO BURST LOCATOR

The Korean Solar Radio Burst Locator (KSRBL) is a spectrometer that can simultaneously observe solar microwave emissions from the chromosphere to the corona over a wide range of frequencies, from 0.245-18 GHz, with a 1 MHz spectral resolution and a 2 s time cadence (Fig. 1). It also has the unique capability of detecting the location of a solar radio burst using a single dish antenna system, which is distinguished from interferometry or mechanical scanning. The burst location can be determined by analyzing the characteristics of spectral modulations caused by the feed, which is located at the focal plane. KSRBL was developed by the Korea Astronomy and Space Science Institute (KASI) in collaboration with the New Jersey Institute of Technology (NJIT), and it was installed at KASI in August 2009.

The KSRBL concept originated with the Solar Radio Burst Locator (SRBL) of NJIT (Dougherty 2000, Dougherty et al. 2000). It had been operated at Owens Valley Radio Observatory (OVRO) between February 1998 and June 2006. Like the SRBL, the KSRBL uses the characteristics of a planar spiral feed to locate burst sources on the Sun, much better than the diffraction limit of KSRBL's 2.1 m antenna, and it has much higher frequency and time resolution than SRBL. In addition, the KSRBL is the first spectrometer to employ the technique of Spectral Kurtosis (SK—Nita et al. 2007) to identify and remove sources of radio frequency interference (RFI) in the radio spectrum. Manmade terrestrial radio signals, such as TV, FM/AM radio, cell phones, radar, and many others, occupy an ever-increasing part of the radio spectrum. Given the continuous frequency coverage of

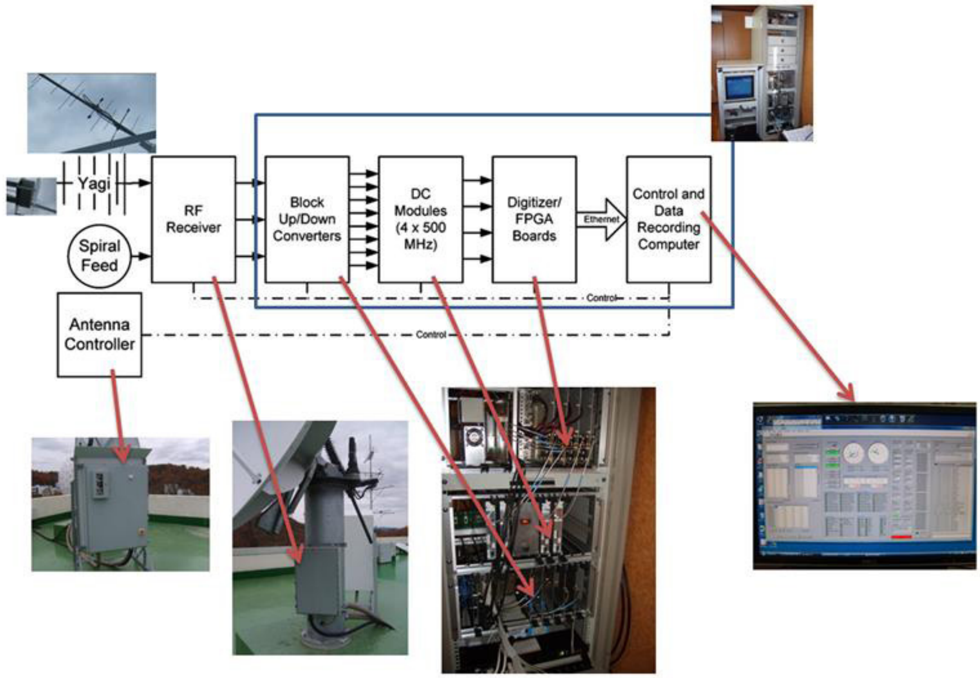

Fig. 2. KSRBL overview block diagram.

KSRBL, these signals are recorded by the instrument and represent unwanted signals that must be removed. Fixed frequencies can be flagged easily, but highly intermittent signals affect the data in subtle ways that are very difficult to find and remove. The SK algorithm is highly sensitive to such intermittent RFI (Dou et al. 2009).

The overview block diagram of the KSRBL is shown in Fig. 2. The KSRBL uses two different feeds. The Yagi, operating at 245 and 410 MHz, is mounted on top of the dish, and the broadband spiral feed, operating from 0.5–18 GHz, is mounted on the focal plane of the dish antenna, which is on the alt-azimuth mount. The signals from the two feeds go to the radio frequency (RF) receiver, where the 0.5–18 GHz band is split into 0.5–9.5 GHz and 9.5–18 GHz bands. Three optical links are used to transmit the signals to the block up/down converters that produce eight bands altogether — four 0.5–1 GHz bands and four 1–5 GHz bands. These eight bands are alternatively switched, four at a time, to provide inputs to four image rejection downconverter modules (DCM), which are computer controlled to further select each 500 MHz bandwidth, single-sideband IF for input to four digital spectrometer boards. The spectrometers digitize the signal to eight bits and implement a polyphase filterbank to provide 2048 subchannels (0.244 MHz resolution) accumulating power and power-squared (for implementing the SK algorithm) with 25 ms time resolution. The power and power-squared data are transmitted via Ethernet to the control and data recording computer, for later processing to eliminate intermittent RFI (Dou et al. 2009).

3. DAILY OPERATION AND CALIBRATION

The KSRBL system is designed for largely unattended operation and remote control via Internet. The control system controls each component and stores and processes data according to a macro-scheduler, and provides the operator with an indication of the health of the system. The macro-scheduler runs a daily sequence of tasks, such as gain calibration at the start of the day and antenna calibration at prescheduled times during the day (typically 4 times a day), and otherwise takes continuous solar data in a standard mode (Fig. 3). The left side of Fig. 3 shows the frequency band sweeping and noise diode status in the standard mode. Each band consists of 2048 frequency channels and each channel is integrated for 25 ms. After four integrations, the band is shifted to cover the full frequency range, and such band sweeping is iterated with the noise diode switched on and off. The noise diode is used for calibration by assuming that its flux, which is added to the input from feeds, is constant. For the calibration process we scale all data with noise diode increase to compensate receiver gain variation.

The data from the four boards are captured by a multi-

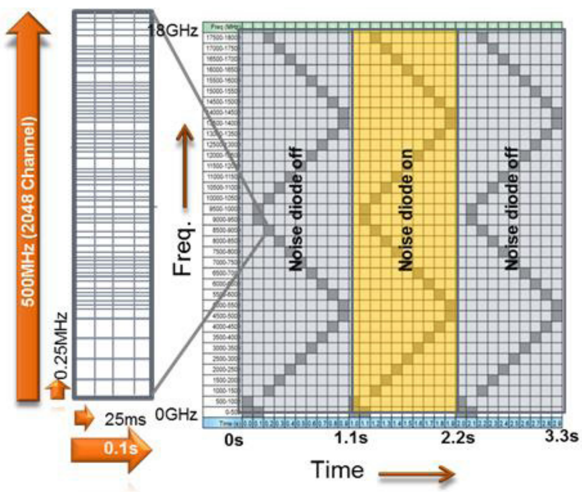

DOY	Time	Task
225	21:38	GAINCAL
225	21:41	TRACKTABLE
225	21:46	SUNRISE
226	00:00	SOLOBS
226	00:20	ANTCAL
226	00:28	SOLOBS
226	02:22	ANTCAL
226	02:30	SOLOBS
226	04:50	ANTCAL
226	05:00	SOLOBS
226	06:32	ANTCAL
226	06:40	SOLOBS
226	09:24	SUNSET
226	09:25	STOW
226	09:26	PROCESS
226	09:26	REWIND
226	09:26	END

Fig. 3. Frequency sampling and daily operation.

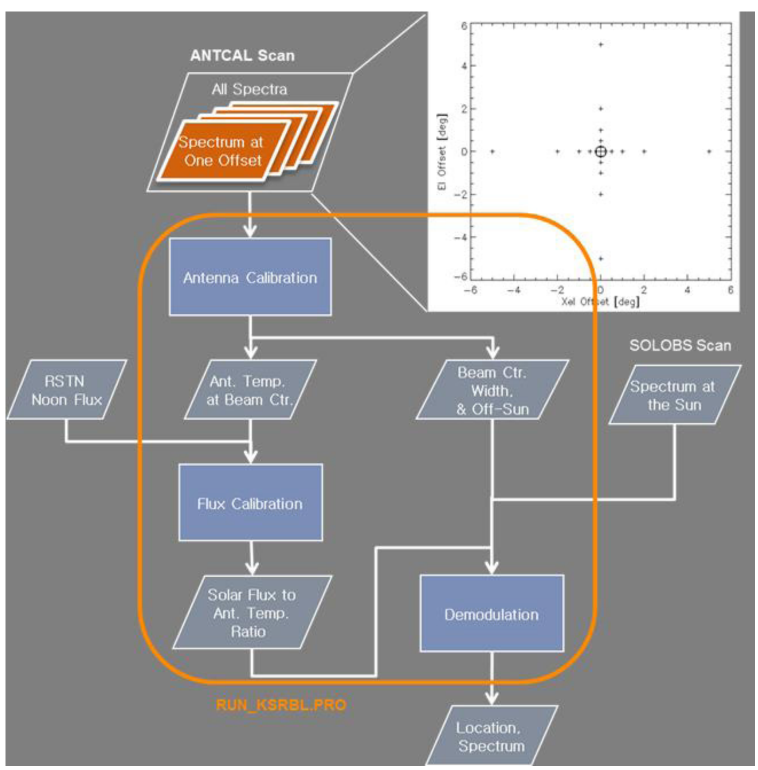

Fig. 4. Calibration process of the KSRBL.

threaded control program implemented in LabVIEW on a standard Windows PC equipped with an Intel quad-core CPU. The four data channels are combined with monitor and control information and saved to disk in a standard, self-describing Lab-VIEW format. The LabVIEW control system includes antenna control, receiver tuning, gain control, system monitoring, and data recording.

The KSRBL calibration includes gain calibration, antenna calibration, flux calibration, and demodulation. We developed the software for the calibration using IDL. Fig. 4 shows how the IDL procedure integrates antenna and flux calibration and demodulation. The system must be well calibrated for both of its essential functions, the location of bursts and the accurate measurement of the solar flux density spectrum.

For gain calibration, we perform a gain calibration task at the beginning of the day during which the front-end attenuation is set to its maximum (35 dB for the spiral feed, and 55 dB for the Yagi) to determine system noise. However the IDL procedure for gain calibration has not yet been developed, and we currently just assume that the system noise is negligible compared to the sky background. The antenna calibration task is done by pointing the dish in a cross pattern with elevation (EL) and cross-elevation (XEL) offsets of 0°, ±0.2°, ±0.5°, ±1.0°, ±2.0°, and ±5.0°. The resulting beam pattern, which is scaled with noise diode increase, is fit with a Gaussian to obtain the center, width, peak flux, and sky background in each axis. In flux calibration, we determine the flux ratio of the measured to the true by comparing each frequency with daily RSTN noon flux.

As the final process, we need demodulation. In this process we calibrate the solar data using the parameters obtained through the previous calibration processes, i.e., we scale data with noise diode increase, subtract sky background, scale with flux ratio, and find the source location as described in Section 4. For the burst spectra, we subtract the quiet Sun spectra before finding the source location.

Fig. 5 shows the dynamic spectrum of the KSRBL on June 7, 2013 as a result of the calibration. It shows the typical characteristics of a microwave radio burst, which is broad in frequencies. We compared this spectrum to NoRP data and it shows a very good correlation with time and frequency (Fig. 6).

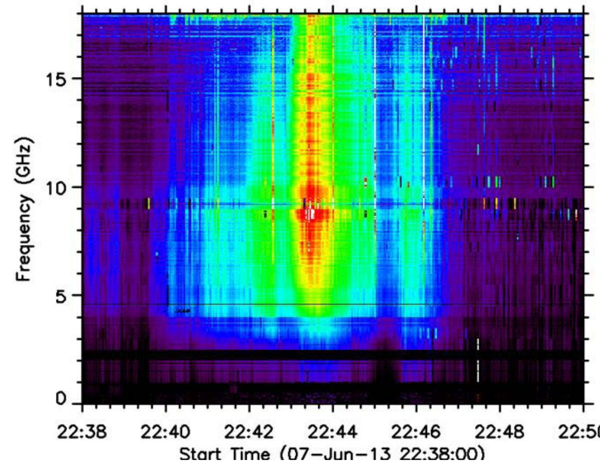

Fig. 5. Dynamic spectrum of the KSRBL on June 7, 2011.

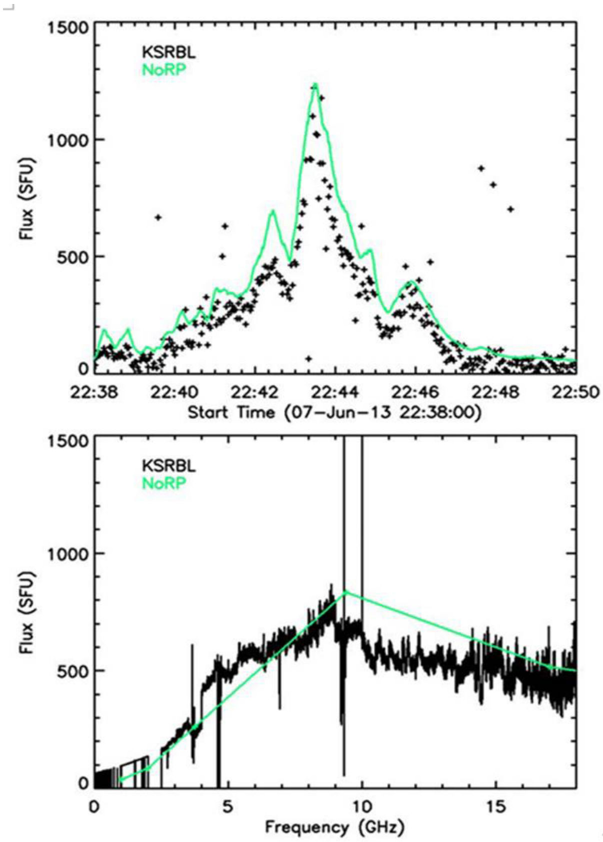

Fig. 6. Correlation of the KSRBL spectrum with NoRP (1 sfu = 10^4Jy = 10^{-22}Wm^{-2} Hz^{-1}).

4. BURST LOCATION

Due to the characteristics of the spiral feed, the beam center varies in a spiral pattern with frequency, making a modulation pattern over the wideband spectrum (Fig. 7). Fig. 8 shows the relationship between the relative intensity and frequency for different burst locations.

The KSRBL operates in Cartesian coordinates referenced to its antenna boresite, with angular units. The effective electrical center of its feed is $(X,Y) = (R\cos\Theta, R\sin\Theta)$, where Θ is the spiral angle (see Fig. 9 for layout details). A point source on the sky at location $(x,y) = (r\cos\theta, r\sin\theta)$ with spectrum $S_0(\nu)$ will produce measured fluxes of $S(\nu) = S_0(\nu)\exp(-\rho^2/2W^2)$ where $\rho^2 = (x-X)^2+(y-Y)^2$ and W is the beam width. R and W are usually inversely proportional to ν. Modulations appear in S due to imbedded Θ dependencies,

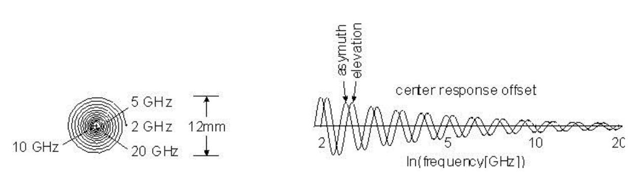

Fig. 7. Left: position of effective electrical center of the SRBL's feed, shown at actual scale (Dougherty 2001).

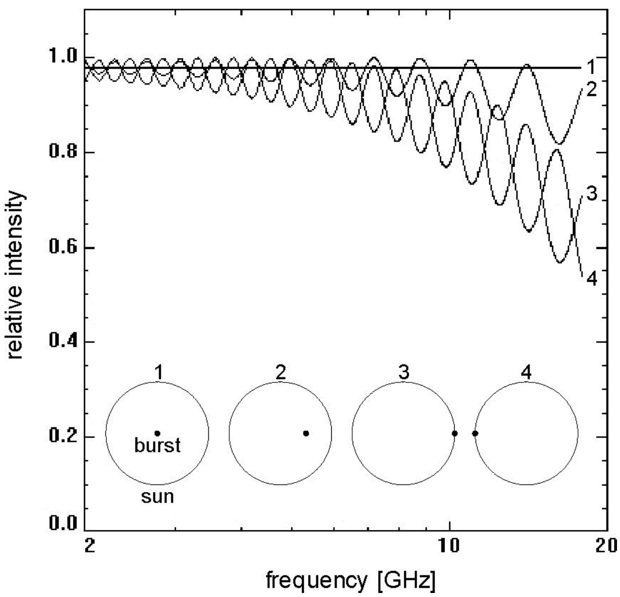

Fig. 8. Relative intensity versus frequency for different burst locations (Dougherty 2001).

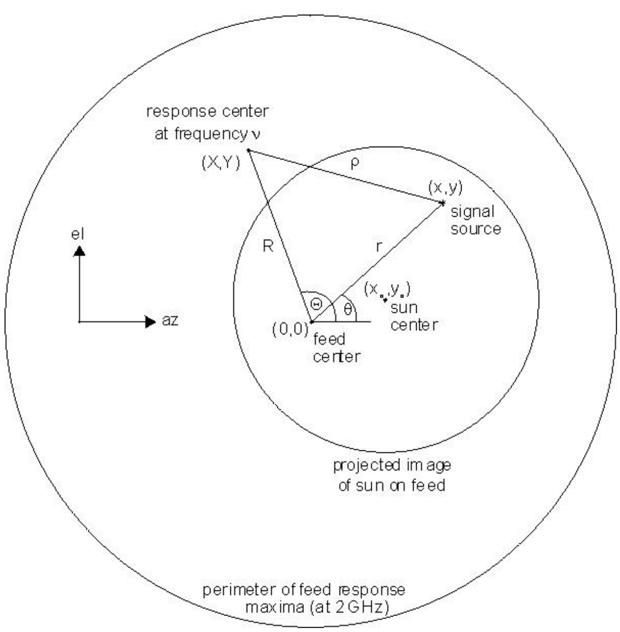

Fig. 9. Focus geometry (Dougherty 2001).

which increase in amplitude with v.

Suppose (X,Y), W, and Θ are known to be functions of frequency through antenna calibration. To find the source location and remove the modulation, we need to extract (x,y), given S. S_0 is not known, but it is presumed to be "smooth" on scales comparable to instrumental modulations. Therefore the function $f = \ln S + [(x-X)^2+(y-Y)^2]/2W^2$ must be free of modulation. To determine (x, y) we start from a presumed initial position (x, y), calculate the function f, fit a smooth curve to f, and evaluate the deviation of the function f from the smooth fit. Then we change the (x, y) and repeat the previous steps, until the deviation is minimized.

Table 1. Solar radio burst event list in 2011

No	Date	Start Time (UT)	X-ray.	Location (KSRBL) (arcsec)	Location (NoRH) (arcsec)	Location (AIA) (arcsec)
1	15-Feb-2011	01:49	X2.2	(233,-244)	(147,-241)	(158,-223)
2	24-Feb-2011	07:30	M3.5	(-720,217)	-	(-900,225)
3	07-Jun-2011	06:13	M2.5	(614,-375)	(702,-363)	(700,-354)
4	04-Aug-2011	03:50	M9.3	(165,308)	(555,206)	(559,185)
5	09-Aug-2011	08:02	X6.9	(879,290)	-	(850,150)

We considered 5 events detected by the KSRBL in 2011 and computed the solar radio burst location on the solar surface using the modulation pattern. To evaluate the results, we used other image data such as Nobeyama Radioheliograph (NoRH) (Nakajima et al. 1994) and Solar Dynamics Observatory (SDO) Atmospheric Imaging Assembly (AIA) (Lemen et al. 2012) (Fig. 10) (Table 1). When both data were available, we compared them with NoRH, as the radio source location could be slightly different from the EUV source location. NoRH didn't have any data on February 24 and August 9, 2011 because it was after sunset. We used AIA data instead in those cases.

In the figure for each event, the red rectangle represents the burst locations over time detected by the KSRBL, and the black cross represents the mean value. The total RMS location error is 215 arcsec but it is 131 arcsec without the event on August 4, 2011, which has an exceptionally large error. On August 4, 2011, we could identify strong RFI in the high frequency bands. Since the higher frequency bands have smaller beam widths, they have larger modulation, and are more sensitive to the source location. We suspect that the strong RFI on August 4 could have affected the exceptionally large error. Excluding the location error on August 4, the result shows that the KSRBL has the ability to locate flaring sources on the Sun typically within about 2' and it exhibits a quite good result as we expected.

To check whether the location error has a systematic bias, we computed the location error on the azimuth and elevation coordinate. Based on the results in Fig. 11, although the number of samples is not high enough, we can roughly conclude the location doesn't have a systematic bias.

5. CONCLUSIONS

The Korean Solar Radio Burst Locator (KSRBL) is designed to provide not only the flux density but also the locations

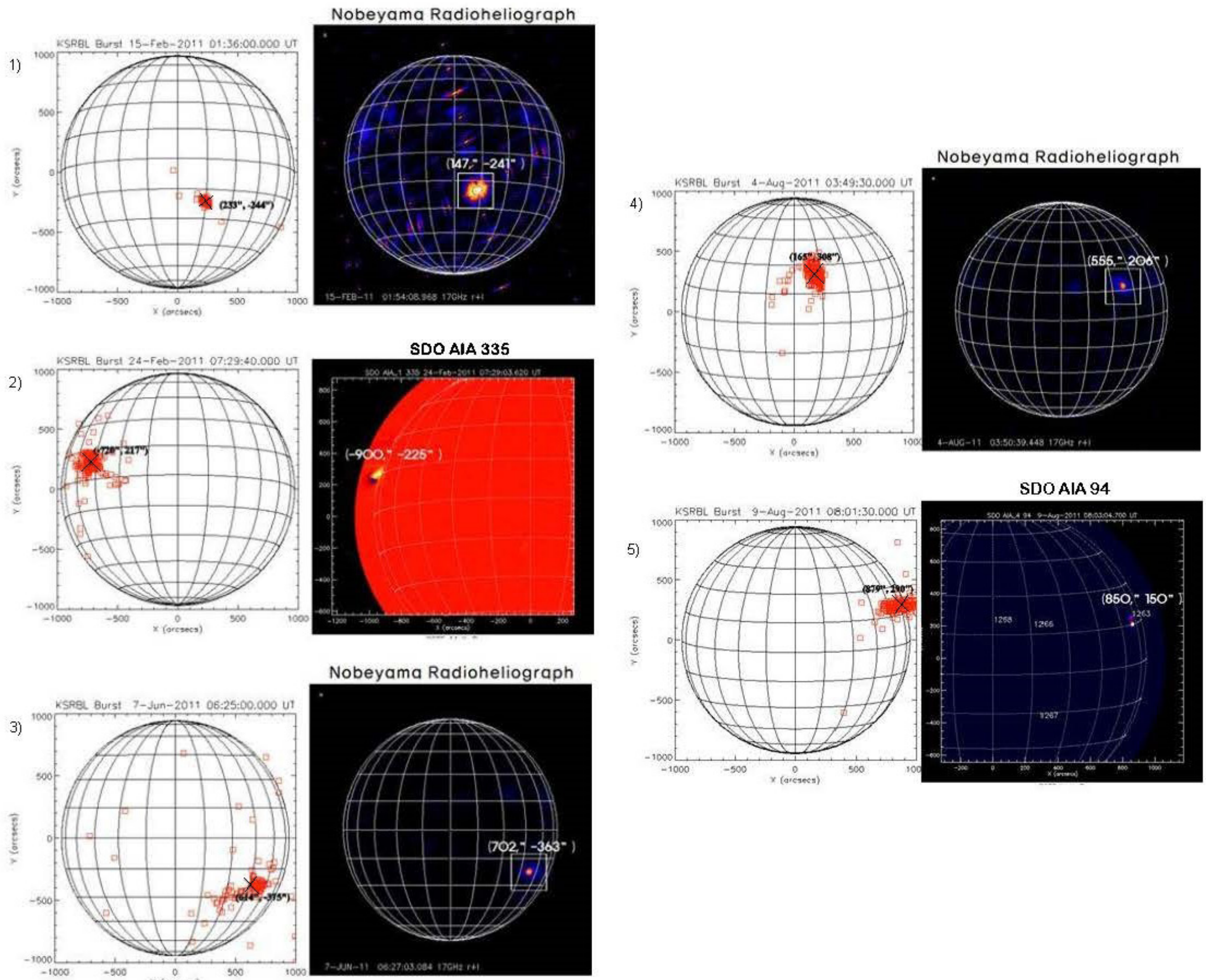

Fig. 10. Solar radio burst location of the KSRBL, NoRH, and AIA.

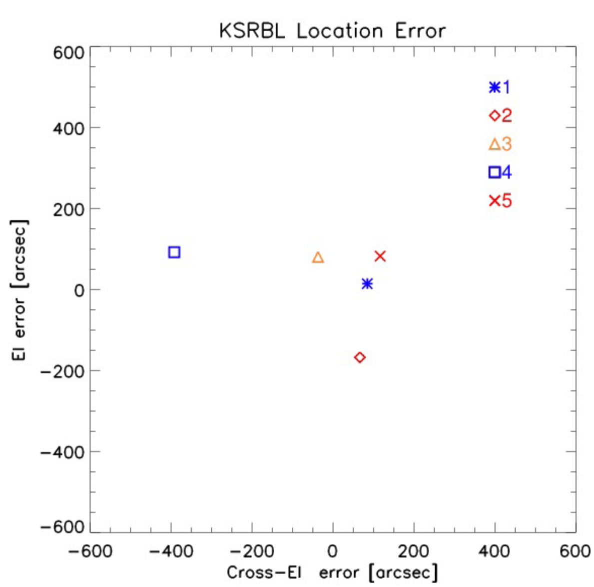

Fig. 11. KSRBL Location error.

of solar radio bursts. The study of solar radio bursts is a key area of research for both basic science and practical applications. The ability of the Sun to release stored magnetic energy within seconds to minutes remains one of the great mysteries of solar physics. This instantaneous energy release appears first in the form of the rapid acceleration (and heating) of charged particles, especially electrons, which then give rise to both radio and X-ray emissions. A better understanding of electron acceleration and transport in solar flares can only be obtained by studying these emissions at high temporal, spectral, and spatial resolution (Dou et al. 2009). Radio emissions from the Sun involve multiple processes of scientific interest (e.g., Bastian et al. 1998), and the high-frequency and time resolutions of the KSRBL, over such a broad range of relevant frequencies, is unprecedented. In a recent study by Hwangbo et al. (2014) on the magnetic structure and nonthermal electrons of flares, the KSRBL has demonstrated superior performance for physical science.

Solar radio bursts can have major effects on technological systems on Earth and in space. Its right-hand circularly polarized (RCP) flux density can directly affect GPS receivers (Cerruti et al. 2008, Carrano et al. 2009). This is why the KSRBL's spiral feed was designed to be RCP, to maximize its usefulness for monitoring potential effects on GPS. Solar radio bursts also accompany other solar activity phenomena, including SEPs, whose effects on Earth and the near-Earth environment depend on the solar longitude of the accompanying flare or CME. Therefore, KSRBL's ability to locate the burst on the Sun, even through rain and clouds, is potentially important for forecasting effects (Dou et al. 2009).

To investigate the effectiveness of operational space weather monitoring, we evaluated the locating capability of the KSRBL. We chose 5 events from 2011 and compared them to NoRH and AIA. As a result, we found that the characteristics of the spiral feed of the KSRBL provided the ability to locate flaring sources on the Sun within around 2′. In a previous study (Hwangbo et al. 2005), we evaluated the same capability of the SRBL at OVRO, which was the prototype of the KSRBL, and the location mean error for single source events was estimated to be about 4.7 arcmin. That result indicates that the KSRBL at KASI has much better location accuracy. It should be noted that the radio burst locations are not always consistent with the flare source location. However, they usually occur within the same flare arcade, which is usually less than 2′. As we can see in Table 1, the source location differences between 17 GHz and EUV are less than about 20 arcsec. These are much smaller than the estimated location errors of the KSRBL and SRBL.

For the future, the KSRBL will provide a broadband view of solar bursts for the purposes of studying solar activity for basic research, and for monitoring solar activity as the source of space weather and solar-terrestrial effects. For the long-term monitoring of solar radio bursts, the system is also important for developing statistics of burst occurrence (Nita et al. 2002, 2004b), for both scientific and engineering goals. For example, using KSRBL data, correlating the distribution of burst statistics with information about the burst location on the solar surface may help to predict the likelihood of occurrence of the largest bursts, and hence the likely impact they might have on specific wireless communication and navigation systems.

ACKNOWLEDGEMENTS

This work was supported by the Operation of the Korean Space Weather Research Center project of KASI.

REFERENCES

Appleton EV, Hey JS, Circular Polarization of Solar Radio Noise, Nature 158, 339 (1946). http://dx.doi.org/10.1038/158339a0

Bala B, Lanzerotti LJ, Gary DE, Thomson DJ, Noise in Wireless Systems Produced by Solar Radio Bursts, Radio Science 37, 1018 (2002). http://dx.doi.org/10.1029/2001RS002481

Bastian TS, Benz AO, Gary DE, Radio Emission from Solar Flares ARA&A 36, 131-188 (1998). http://adsabs.harvard.edu/abs/1998ARA%26A..36..131B

Bastian TS, The Frequency Agile Solar Radiotelescope, Solar and Space Weather Radiophysics 314, 47-69 (2005). http://dx.doi.org/10.1007/1-4020-2814-8_3

Carrano CS, Bridgwood CT, Groves KM, Impacts of the December 2006 solar radio bursts on the performance of GPS, Radio Science 44, RS0A25 (2009). http://dx.doi.org/10.1029/2008RS004071

Cerruti AP, Kintner Jr. PM, Gary DE, Lanzerotti LJ, de Paula ER, et al., Observed solar radio burst effects on GPS/Wide Area Augmentation System carrier-to-noise ratio, Space Weather 4, S10006 (2006). http://dx.doi.org/10.1029/2006SW000254

Cerruti AP, Kintner Jr. PM, Gary DE, Mannucci AJ, Meyer RF, et al., Effect of intense December 2006 solar radio bursts on GPS receivers, Space Weather 6, S10D07 (2008). http://dx.doi.org/10.1029/2007SW000375

Dierckxsens M, Tziotziou K, Dalla S, Patsou I, Marsh MS, et al, Relationship between Solar Energetic Particles and Properties of Flares and CMEs: Statistical Analysis of Solar Cycle 23 Events, SoPh 290, 841-874 (2015). http://dx.doi.org/10.1007/s11207-014-0641-4

Dou Y, Gary DE, Liu Z, Nita GM, Bong SC, et al., The Korean Solar Radio Burst Locator (KSRBL), PASP 121, 512-526 (2009). http://dx.doi.org/10.1086/599624

Dougherty BL, A comparison of flux measurements, location results, an timing reports for several simultaneously recorded large solar microwave bursts from RSTN, SOON, and the SRBL prototype at OVRO, California Institute of Technology, (2000).

Dougherty BL, Freely WB, Zirin H, Gary DE, Hurford GJ, Solar Radio Burst Locator, eds. Ramaty R, Mandzhavidze N (Astronomical Society of the Pacific, San Francisco, 2000), 367-370.

Dougherty BL, Technical Review of the Solar Radio Burst Locator, California Institute of Technology, (2001).

Feynman J, Gabriel SB, On space weather consequences and predictions, JGR 105, 10543-10564 (2000). http://dx.doi.org/10.1029/1999JA000141

Fu Q, Ji H, Qin Z, Xu Z, Xia Z, et al., A New Solar Broadband Radio Spectrometer (SBRS) in China, SoPh 222, 167-173 (2004). http://dx.doi.org/10.1023/B:SOLA.0000036876.14446.dd

Gary DE, Lanzerotti LJ, Nita GM, Thomson DJ, Effects of Solar Radio Bursts on Wireless Systems, Effects of Space Weather on Technology Infrastructure 176, 203-213 (2004). http://dx.doi.org/10.1007/1-4020-2754-0_11

Guidice DA, Cliver EW, Barron WR, Kahler S, The Air Force RSTN System, BAAS 13, 553 (1981).

Hwangbo JE, Bong SC, Cho KS, Moon YJ, Lee DY, et al., An Evaluation of The Solar Radio Burst Locator (SRBL) at OVRO, JKAS 38, 437-443 (2005). http://dx.doi.org/10.5303/JKAS.2005.38.4.437

Hwangbo JE, Lee J, Park SH, Kim S, Lee DY, et al., Magnetic Structure and Nonthermal Electrons in The X6.9 Flare on 2011 August 9, ApJ 796, 80 (2014). http://dx.doi.org/10.1088/0004-637X/796/2/80

Lemen JR, Title AM, Akin DJ, Boerner PF, Chou C, et al., The Atmospheric Imaging Assembly (AIA) on the Solar Dynamics Observatory (SDO), SoPh 275, 17-40 (2012). http://dx.doi.org/10.1007/s11207-011-9776-8

Messmer P, Benz AO, Monstein C, PHOENIX-2: A New Broadband Spectrometer for Deci- metric and Microwave Radio Bursts - First Results, SoPh 187, 335-345 (1999). http://dx.doi.org/10.1023/A:1005194314845

Nakajima H, Sekiguchi H, Sawa M, Kai K, Kawashima S, et al., The The radiometer and ploarimeters at 80, 35, and 17GHz for solar observations at Nobeyama, Publ.Astron. Soc.Japan 37, 163-170 (1985). http://adsabs.harvard.edu/abs/1985PASJ...37..163N

Nakajima H, Nishio M, Enome S, Shibasaki K, Takano T, et al., The Nobeyama radioheliograph, Proc. of IEEE 82, 705-713 (1994). http://adsabs.harvard.edu/abs/1994IEEEP..82..705N.

Nita GM, Gary DE, Lanzerotti LJ, Thomson DJ, The Peak Flux Distribution of Solar Radio Bursts, AJ 570, 423-438 (2002). http://dx.doi.org/10.1086/339577

Nita GM, Gary DE, Lanzerotti LJ, Statistics of Solar Microwave Radio Burst Spectra with Implications for Operations of Microwave Radio Systems, Space Weather 2, S11005 (2004a). http://dx.doi.org/10.1029/2004SW000090

Nita GM, Gary DE, Lee J, Statistical Study of Two Years of Solar Flare Radio Spectra Obtained with the Owens Valley Solar Array, ApJ 605, 528-545 (2004b). http://dx.doi.org/10.1086/382219

Nita GM, Gary DE, Liu Z, Hurford GJ, White SM, Radio Frequency Interference Excision Using Spectral-Domain Statistics, PASP 119, 805-827 (2007). http://dx.doi.org/10.1086/520938

Park J, Moon YJ, What flare and CME parameters control the occurrence of solar proton events?, JGR 119, 9456-9463 (2014). http://dx.doi.org/10.1002/2014JA020272